Electromagnetic imaging of gas hydrate deposits off-shore Taiwan: First results of the Taiflux survey

Andrei Swidinsky[1)], Malte Sommer[2)], Sebastian Hölz[2)], Marion Jegen[2)], Christian Berndt[2)] & Wu Chi[3)]*
[1)] *Colorado School of Mines Department of Geophysics*
[2)] *GEOMAR Helmholtz Centre for Ocean Research Kiel*
[3)] *Institute of Earth Sciences, Academia Sinica, Taipei, Taiwan*

Summary

We present the first results of an electromagnetic survey for gas hydrates offshore Taiwan using a novel marine controlled-source electromagnetic system. Seismic evidence suggests the presence of gas hydrates and free gas in both accretionary (*Four-Way-Closure*) and erosional (*Formose Ridge*) settings to the southwest of the island, but complementary geophysical techniques are required to further quantify the distribution and concentration of the deposits. Electromagnetic experiments were conducted along profiles in both regions and show an increase in apparent resistivity at depth, which may be associated with the presence of methane hydrates. However, both profiles are characterized by severe bathymetric relief, in some cases having slope angles greater than 30 degrees, such that the apparent resistivity section may be biased by tilts of the instruments. We therefore derive a first-order bathymetric correction which can be applied to apparent resistivities and tested the correction procedure on data collected at *Four-Way-Closure*. Results show that increased apparent resistivities persist and reach up to 7Ωm, which suggests the presence of significant concentrations of hydrate or free gas at this location.

Introduction

The existence of gas hydrates offshore Taiwan has been inferred from a suite of seafloor observations and geophysical data sets (Liu et al. 2006) and stirred national Taiwanese interest to explore methane hydrates as a potential energy source. In collaboration between Germany and Taiwan, "Taiflux", a joint five-week geophysical cruise on the German research vessel Sonne (cruise SO227) was staged in Spring of 2013. The overall goal was to map and understand the gas and fluid flow systems responsible for hydrate formation in two work areas (Figure 1). The *Formosa Ridge* work area is located on the passive continental margin in an erosional setting, whereas the *Four-Way-Closur*e site is located on the active margin in an accretionary setting. Here we will report on first results of the latter work area. The specific aim of the experiment was to map and quantify in detail methane hydrates and free gas within the sediments for these settings, information that is vital to understand the fluid and gas migration systems but also for energy resource assessment.

Method

Measurements were carried out with a novel marine electromagnetic transmitter system with two transmitter polarizations (see Hölz et al., 2014 or Swidinsky et al., 2014). The transmitter is operated over the ship's winch cable in a pogo-style manner: as the transmitter is placed onto the seafloor, it mechanically unfolds four arms which form two orthogonal, 10m-long dipoles. This allows for the transmission of two perpendicular source polarizations. Conventional nodal receivers measure the two orthogonal horizontal components of the electric field (Figure 2, top). The transmitter is then lifted up and moved to the next position.

Each transmitter-receiver pair has four electric field measurements: two orthogonal electric field components recorded from each of the two orthogonal dipole transmissions. Swidinsky et al. (2013) describe a method to simplify the dataset by reducing the four electric field measurements from each transmitter-receiver pair to a single, rotationally invariant quantity. This invariant is then further reduced into an apparent resistivity, which can be used to create an apparent resistivity pseudosection, analogous to a DC resistivity pseudosection. To summarize the approach: the four electric fields are arranged in a matrix and the determinant of this matrix is invariant with respect to transmitter or receiver rotation. This invariant step-response is then differentiated with respect to logarithmic time to produce an invariant pseudoimpulse response, and the bulk arrival time of this response is converted to an apparent halfspace resistivity ρ_a by the relationship

$$\rho_a = \frac{\mu_o r^2}{4\tau}, \qquad (1)$$

where μ_o is the magnetic permeability, r is the transmitter-receiver distance, and τ is the arrival time picked directly from the pseudoimpulse response data. Each apparent resistivity ρ_a can be plotted at the midpoint of each transmitter-receiver pair at a pseudodepth corresponding to half the transmitter-receiver offset, to produce an apparent resistivity pseudosection for rapid mapping and first pass interpretation.

DOI http://dx.doi.org/10.1190/segam2014-0100.1

The theory outlined in Swidinsky et al. [2013] is only strictly valid when the transmitter and receiver lie flat on the seafloor in the same plane. In the case of the Taiflux survey, the severe bathymetry resulted in some instruments which were tilted in excess of 30 degrees, violating the assumptions of the theory developed to produce apparent resistivity maps. With some careful trigonometry, the invariant response can be calculated in a wholespace for a generally rotated situation using the analytic expression (2.50) in Ward & Hohmann (1988). In a wholespace, equation (1) should recover the true resistivity when there are no tilts or altitude differences between the instruments. Figure 3 shows the apparent resistivity for a range of transmitter and receiver pitch angles in a wholespace of resistivity 2Ωm. Note that this resistivity can be as much as 15% in error for severe tilts. Figure 4 shows the general geometry used for the calculation when the transmitter and receiver dipoles can be tilted at an arbitrary angle.

The field instrumentation used during the Taiflux experiment records the heading of the transmitter and each receiver, along with their pitch, roll and depth on the seafloor. With this information, we can correct the apparent resistivity derived by equation (1) for the first-order effects of tilted instruments. Note that the change in apparent resistivity in a wholespace is independent of the conductivity as the change in peak arrival time is a purely geometrical effect, produced by unwanted vertical-vertical coupling of the transmitter to the receiver. Therefore, the correction term we propose is purely geometric and model independent. We assert that the conductivity contrasts produced by bathymetry and subsurface structure are higher order effects and the most severe distortions of the apparent resistivity are produced by geometry. In a conceptual sense, the tilt correction we propose is similar to the free-air or latitude correction in a gravity survey, which only considers the geometry of the experiment and not the density of the subsurface.

Real data from Taiflux

Figure 5 (top) shows an uncorrected apparent resistivity pseudosection along the survey line shown in figure 2. The transmitter-receiver midpoint where each apparent resistivity is plotted is shifted according to the water depth at that point. Therefore the pseudosection follows the bathymetric profile but has been derived assuming that the transmitter and receiver are untilted and on the same plane. Note that there is a significant increase in apparent resistivity at the west end of the line beneath the ridge, which may indicate the presence of large quantities of free gas and gas hydrate. However, the bathymetry along this section of the profile is particularly steep and severe tilts were recorded at many transmitter and receiver stations. Instruments landing on outcropping carbonate blocks were even more affected (one transmitter station had a pitch of 38 degrees). It is therefore questionable at this stage of imaging if the anomaly is indeed caused by geology or is simply an acquisition footprint of the survey.

Figure 5 (middle) shows the geometrically corrected apparent resistivity pseudosection. For each transmitter receiver pair, a correction factor was derived from the pitch and roll of each instrument, along with their depths on the seafloor and their headings. The resistivity anomaly is still present in the pseudosection and in some cases is actually amplified to values as high as 7Ωm. It is still possible that the anomaly is an artifact of the conductivity contrast produced by the bathymetry, but given the high porosity of the shallow sediments and the consequent similarity in conductivity between seawater and seafloor, it is unlikely a bathymetric effect could cause such a significant increase in apparent resistivity. The development of a second order, Bouguer-like correction might be possible to account for this bathymetric effect but is beyond the scope of the present paper.

The increased apparent resistivities suggest that significant quantities of hydrate are present beneath the ridge at the *Four-Way-Closure*. This is in agreement with high resolution 3D seismic evidence of hydrate accumulations in the area (Berndt, 2013), where a strong BSR underlies numerous high amplitude reflectors in the lower section of the gas hydrate stability zone. Figure 5 (bottom) shows a comparison of methods by overlaying the resistivity image on a 1500m/s depth-converted seismic section in figure 5.

Conclusions

We have presented an apparent resistivity image of a hydrate deposit offshore Taiwan, and have developed a first-order correction method to account for significant instrument tilts. Results show increased apparent resistivities beneath an active ridge setting which may indicate high concentrations of free gas or gas hydrate. The tilt correction method we describe here can be easily applied to field data in order to produce more reliable maps of apparent resistivity in areas of rough bathymetry. However, 3D interpretation (e.g. Sommer et al. 2013) would be needed to obtain a more accurate resistivity image of the sediments. Such a method can naturally handle arbitrary instrument geometry and therefore the correction we describe here is most suitable for the rapid creation of apparent resistivity images.

Acknowledgments

This work was supported by through the GEOTECHNOLOGY programme, project SUGAR-A, grant no. 03G0687.

DOI http://dx.doi.org/10.1190/segam2014-0100.1

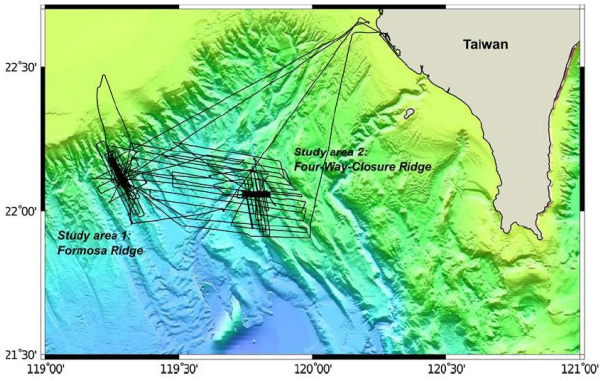

Figure 1: Bathymetric map with cruise track of the German RV Sonne (SO227, 2.4.2013 Kaohsiung – 2.5.2013 Kaohsiung). Geophysical experiments to image fluid flow and methane hydrates were carried out in two target areas representing an passive erosional setting (Formosa Ridge) and an active accretionary setting (Four-Way-Closure).

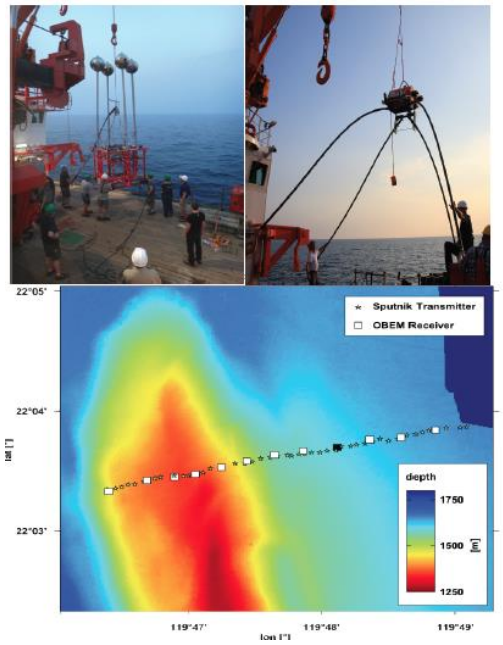

Figure 2: Top: time domain electromagnetic instrumentation: Left panel shows the transmitter, which consists of two orthogonal dipoles that unfold to a length of 10 m when the system is placed on seafloor. The transmitter signal consists of a bi-polar square wave of 50A and a 50% duty cycle. The transmitter is placed on the seafloor, delivers a transmission cycle and is then moved to the next station. Right panel shows one of the 12 electromagnetic receivers which were placed on the seafloor sample the electric field at 10 kHz by two orthogonal dipoles. Bottom: the CSEM profile across the Four-Way-Closure

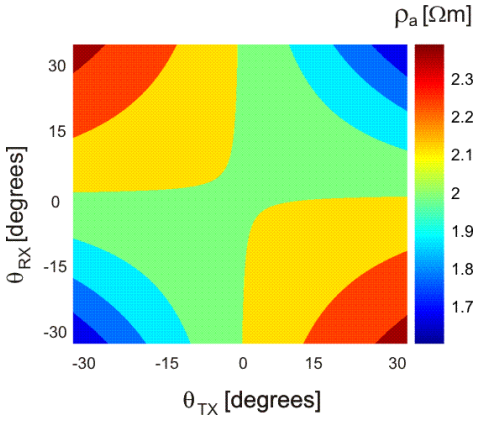

Figure 3: The apparent resistivity, calculated using equation (1), when all angles are zero except for the pitch of TX1 and RX1. The true resistivity of the wholespace is 2Ωm. When either transmitter or receiver is not tilted, the apparent resistivity is equal to the true resistivity.

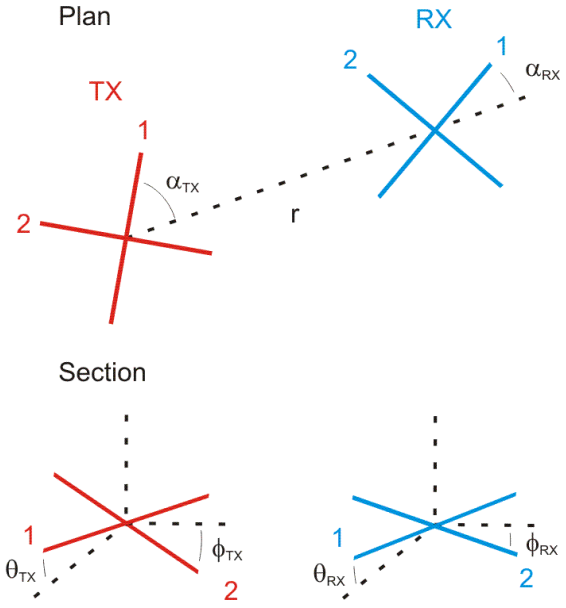

Figure 4: The geometry of a tilted transmitter and receiver pair in a wholespace. Plan view: the angles α_{RX} and α_{TX} denote the heading of transmitter 1 and receiver 1 with respect to the horizontal distance *r* joining the two instruments. Section view: the angles θ_{TX} and ϕ_{TX} denote the pitch of the 1st and 2nd transmitter dipole with respect to the horizontal, while the angles θ_{RX} and ϕ_{RX} denote the pitch of the 1st and 2nd receiver dipole. (Note that each instrument is drawn in its own coordinate system. Also note that ϕ_{TX} and ϕ_{RX} are both negative in this sketch). The geometry can be extended to the case where transmitter and receiver are at different altitudes by incorporating the altitude difference into the distance *r* and modifying the tilt angles.

DOI http://dx.doi.org/10.1190/segam2014-0100.1

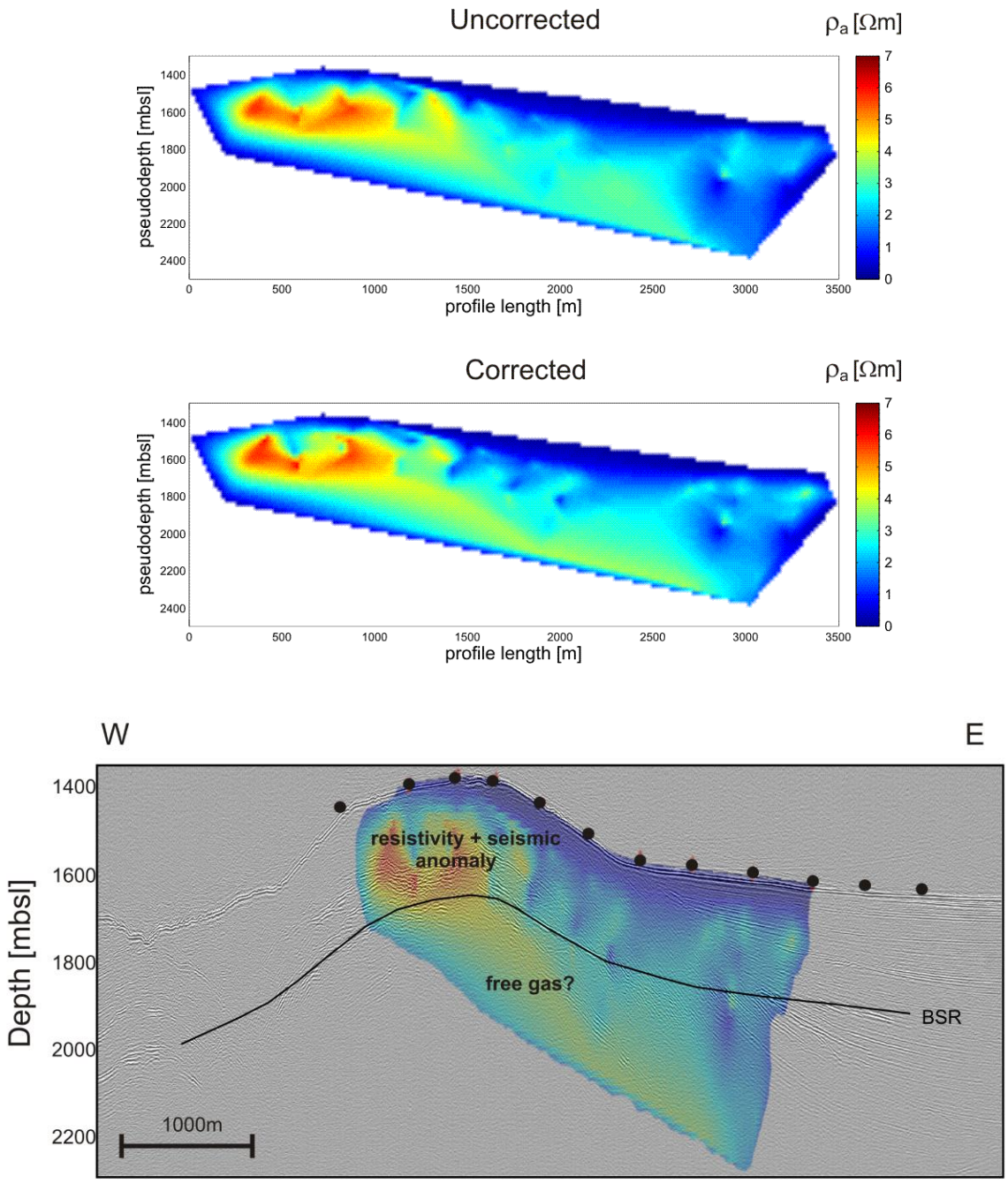

Figure 5: Top: the interpolated, uncorrected apparent resistivity pseudosection, superimposed on the seafloor bathymetry. Middle: the geometrically corrected, interpolated apparent resistivity pseudosection. Bottom: overlay of the resistivity model onto a high resolution seismic image of Four-Way-Closure. Note that vertical exaggeration has been applied to the seismic image and corresponding resistivity overlay, and that we have assumed the depth of investigation of the CSEM system is half the transmitter-receiver offset. Solid circles are receiver positions.

DOI http://dx.doi.org/10.1190/segam2014-0100.1

http://dx.doi.org/10.1190/segam2014-0100.1

EDITED REFERENCES

Note: This reference list is a copy-edited version of the reference list submitted by the author. Reference lists for the 2014 SEG Technical Program Expanded Abstracts have been copy edited so that references provided with the online metadata for each paper will achieve a high degree of linking to cited sources that appear on the Web.

REFERENCES

Berndt, C., ed., 2013, RV Sonne Fahrtberight/Cruise Report SO227 Taiflux: Fluid and gas migration in the transition from a passive to an active continental margin off SW Taiwan, 02.04.–02.05.2013, Kaohsiung-Kaohsiung (Taiwan): GEOMAR Report, N. Series 011, doi: 10.3289/GEOMAR_REP_NS_11_2013.

Hölz, S., A. Swidinsky, and M. Jegen, 2014, Investigations on small scale targets with Sputnik, a two polarization transmitter system: 76th Conference & Exhibition Workshop, EAGE, Extended Abstracts, WS9-A05.

Liu, C. S., P. Schnurle, Y. Wang, S. H. Chuang, S. C. Chen, and T. H. Hsiuan, 2006, Distribution and characters of gas hydrate offshore of southwestern Taiwan: Terrestrial, Atmospheric and Oceanic Sciences, **17**, 615–644.

Sommer, M., S. Hölz, M. Moorkamp, A. Swidinsky, B. Heincke, C. Scholl, and M. Jegen, 2013, GPU parallelization of a three dimensional marine CSEM code: Computers & Geosciences, **58**, 91–99, http://dx.doi.org/10.1016/j.cageo.2013.04.004.

Swidinsky, A., S. Hölz, and M. Jegen, 2013, Rapid resistivity imaging using a transient marine CSEM survey with two transmitter polarizations: 75th Conference & Exhibition, EAGE, Extended Abstracts, TU 11 11.

Swidinsky, A., S. Hölz, M. Sommer, M. Jegen, K. Weitemeyer, and C. Berndt, 2014, First results from an electromagnetic survey of gas hydrate deposits offshore mid-Norway: 76th Conference & Exhibition, EAGE, Extended Abstracts, Tu E108 12.

Ward, S. H., and G. W. Hohmann, 1988, Electromagnetic theory for geophysical applications, *in* M. N. Nabighian, ed., Electromagnetic methods in applied geophysics: SEG, 131–311.